# A theoretical approach for the reduction of X-ray radiation dose within the optimization of the tomographic scanning process

**A Ozdiev and S Lazarev**

National Research Tomsk Polytechnic University, Tomsk, Russia

ozdiev@tpu.ru

**Abstract.** X-ray tomography is one of the widespread methods of medical diagnostics. Modern medical tomographic setups have many advantages among them high resolution, high level of reproducibility, the simplicity of utilization, and many others. However, one of the most significant challenges of this method is a reducing of the radiation dose. We propose here an alternative scanning approach and an optimized filtered backprojection algorithm as a tool for the dose reduction by lower illumination area during the scan. Further, we demonstrate the power of this approach for dental application, where tomographic visualization is used as the main diagnostics instrument, employing a 3D model of a skull with teeth. From the results of our reconstruction, different defects in the teeth are successfully detected with an acceptable resolution. We hope that the proposed approach will be used as a fundamental idea to low the radiation dose in medical computer topology.

## 1. Introduction

Since the material-penetrating X-rays were discovered by Roentgen in 1895 many technological breakthroughs based on this phenomenon were made [1-4]. Material and geology science, industrial non-destructive control, and medical diagnostics moved to a radically new level due to opportunities provided by X-ray imaging [5]. Among others, computed tomography (CT) as a good example provided access to three-dimensional information about specimens with a high spatial resolution [6]. Medical diagnostics in contrast to other applications of X-ray imaging have much more limitations in terms of clinical utilization [7]. One of the most critical challenges is the reduction of the radiation dose received by a patient during the imaging procedure. Patients with a complex disease such as cancer must regularly go through the diagnostic procedure in purpose to control the current state of the tumor. However, in many cases, this inspection is impossible since the medical equipment does not fulfill requirements for radiation dose regarding utilization for periodical diagnostics procedures. The mean values of the effective dose by standard and low-dose studies for different body parts [8] are presented in Table 1. At the same time, the reference dose level recommended for a group of X-ray studies conducted for diagnostic purposes is about 15 millisieverts (mSv) per year. The dose problem is especially critical in the case of scans of a head and dental area due to the importance of this organ for life. Therefore, the dose of the medical CT scans of a head must be reduced as much as possible (Table 1). Limitations for human annual effective radiation dose are shown in Table 1.

Here we report on a modification of the tomographic scanning geometry with a purpose to reduce the received by a specimen dose in CT. Additionally, we present an optimized reconstruction algorithm

to reconstruct objects from the data obtained with this geometry. The power of the method is demonstrated for the dental cone X-ray beam CT on a three-dimensional (3D) model of a human skull.

**Table 1.** Limitations for human annual effective radiation dose.

|  | Effective dose (mSv) according to imaging area | | | |
|---|---|---|---|---|
|  | head | chest | abdomen | pelvis |
| Standard | 1.83 | 6.04 | 11.47 | 11.47 |
| Low-dose | 1.46 | 4.41 | 1.86 | 3.18 |

## 2. Method

The first There are three parameters, which define the dose received by an object: the X-ray beam intensity, exposure time, and the illuminated by X-rays area. Usually, it is necessary to investigate only a part of the specimen, which is called a region of interest (ROI). However, the commonly used in CT general filtered backprojection algorithm (FBA) [9] requires the center of the investigated object to be on the optical axis of the setup [10]. Therefore, the X-ray beams should illuminate not only the ROI but the whole object, even if the ROI is close to the edge of the sample. Our idea of the radiation dose reduction is based on the decreased illuminated area, while the exposure time and the X-ray beam intensity are fixed. We propose to slit or to collimate the X-ray beam and to shift it to be focused precisely on the ROI and to optimize the reconstruction algorithm for this case. Thus, the affected radiation dose will be proportionally decreased with the exposed area compare to the standard CT scan. In order to develop the proposed scanning algorithm, we, first, used a simple phantom with a shifted ROI. Schematic representation of the phantom and the proposed approach is shown in Figure 1. Since we aim to apply the proposed method to dental scans, the simple phantom mimics a slice of a skull with teeth. Instead of teeth, different geometric figures are used with the aim to reconstruct their shapes and positions (Figure 1). We introduce a Cartesian coordinate system xyz with the x-axis parallel to the central X-ray beam of the cone radiation sources, and the 2D model is located in the xy-plane. In case of the standard CT scan, the whole sample would be illuminated by the uncollimated X-ray beam from a source «$S_u$» presented in Figure 1. Our approach involves, in contrast, a collimated source «$S_c$» and only the central part of the ROI is illuminated. The center of the test sample «O» is still on the optical axis of the setup (Figure 1).
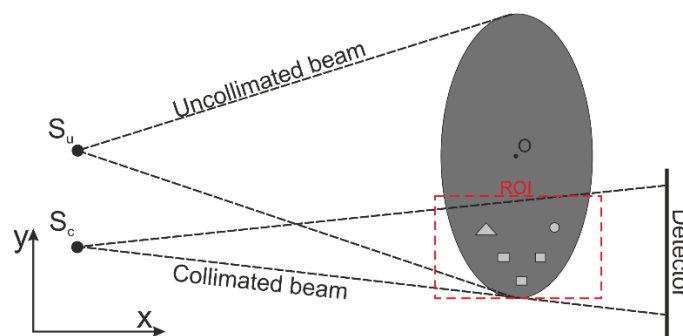


**Figure 1.** Schematic representation of the simple 2D phantom and the proposed scanning approach.

The 2D phantom is in the xy-plane of the Cartesian coordinate system xyz with the x-axis parallel to the central X-ray beam of the cone radiation sources. In case of the standard CT scan with the uncollimated X-ray beam from a source "$S_u$", the whole sample is illuminated. In the proposed approach, a collimated source "$S_c$" reduces the illuminated area only to the central part of the ROI of the specimen. The center of the sample is marked as "O" and is on the optical axis of the setup in both scans

The standard FBA algorithm, in this case, cannot be applied for the reconstruction from the proposed scanning geometry [11]. Therefore, the algorithm should be optimized taking into account all new condition of the scan. Mathematically, the backprojection operation is defined as [12]

$$f_{BP}(x,y) = p \cdot (x \cdot cos\varphi + y \cdot sin\varphi)d\varphi \qquad (1)$$

where $p$ is the Radon transform of $f_{BP}$, and $\phi$ is the rotation angle. However, geometrically the backprojection operation only propagates the measured sinogram back into the image space along the projection path. Thus, in the case of the beam collimation, the measured sinogram also should be propagated back along the exact initial projection path. For that purpose, the distance between the origin and the individual ray should be considered as following

$$f_{BP}(x,y) = p \cdot (x \cdot cos\varphi + y \cdot sin\varphi - s)d\varphi \qquad (2)$$

where $s$ is the length of the perpendicular from the given ray to the origin, which is still matched with the center of rotation for the collimated X-ray beam case.

In order to prove the reliability of the proposed algorithm, corresponding numerical simulation was performed. First, we simulated the proposed tomographic experiment with the discussed scanning geometry. The phantom in Figure 1 was used for the simulations. The virtual measurements were done based on the ray casting technique [13] within the developed Python software. The sample was scanned from 0 to 180 degrees with a step of one degree. The beam was considered as the set of rays and trajectories of each ray was calculated for every rotational angle. Then the sinogram was measured by accumulating the object projections for all angular positions and is presented in Figure 2(a). The reconstruction of the scanned part of the sample (ROI) using the proposed algorithm is shown in Figure 2(b). Comparison of the reconstruction (see Figure 2(b)) with the initial 2D phantom (see Figure 1) allows us to conclude on a success of the algorithm. Both positions and the shapes of the geometric objects of the phantom were reconstructed with a reasonable resolution.

The collimated X-ray beam width used in the simulated was three times smaller than the width of the uncollimated beam in case of the illumination of the whole phantom. Therefore, if the sample is considered to be homogeneous, the exposure time and the beam intensity are the same, the overall radiation dose decreases approximately three times or for 60%. Despite the 2D model involved in our discussion, the algorithm could be extended to the 3D case based on the Feldkamp tomographic reconstruction algorithm [14]. Figure 3 demonstrates this 3D approach with a 3D phantom. The main idea is that any 3D phantom should be interpreted as a set of 2D slices originating from the planes consisting lines with columns of the detector pixels and the point X-ray source as it is shown in Figure 3. Each slice, in this case, could be analyzed as it was discussed above and the final 3D reconstruction could be constructed from the 2D reconstructions. This method will be used further in order to reconstruct a more realistic 3D model.
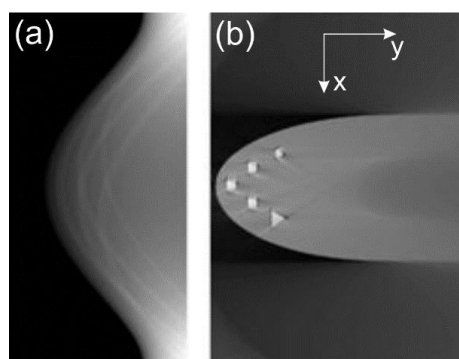


**Figure 2.** Reconstruction results of the 2D phantom. From the sinogram of the scan from 0 to 180 degrees with a one-degree step (a), the successful reconstruction of the sample (b) was obtained using the modified algorithm.
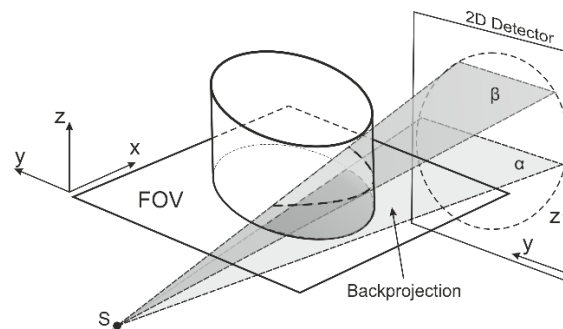
**Figure 3.** The 3D case of the proposed scanning approach. The X-ray beam cone is assumed as an ensemble of planes pathing through the X-ray source "S" as it is shown in the figure. Two planes are shown as an example: the plane α, which coincides with the xy-plane and the plane β.

## 3. Results

To demonstrate the performance of the proposed scanning approach and the optimized reconstruction algorithm in 3D on a realistic phantom, we employed a 3D model of the human skull presented from different directions in Figure 4. We defined a Cartesian coordinate system xyz shown in the figure.
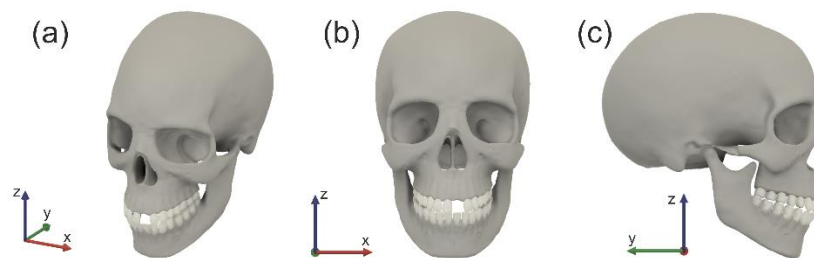


**Figure 4.** The 3D test object in the form of a skull with teeth, which was used for the numerical simulation. Figures (a), (b), and (c) are different views of the model.

In this simulation, we aim to mimic the dental cone X-ray beam CT of the facial bones and to reconstruct the teeth in 3D without illumination of the cranium bones (cranial vault). For the simplification, teeth in the upper jaw of the skull were used and were isolated in a separate 3D volume presented in Figures 5(a-d). To analyze the capability and resolution of the method, different defects were introduced in the model of the teeth. The largest one is a missing tooth in the central part of the model. Further, two teeth have planar defects, which are visible in Figure 5(c).
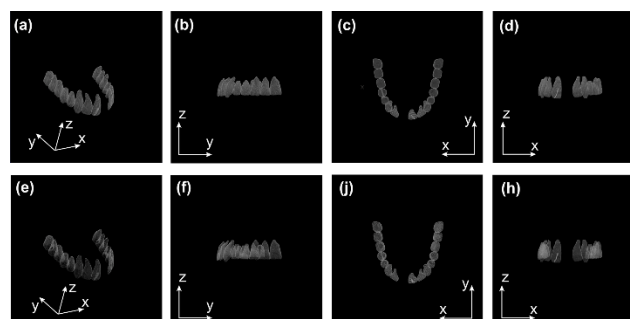


**Figure 5.** View from different directions of the 3D model of the teeth in the upper jaw from the 3D skull, which was used as an experimental object for the numerical simulations (a-d). The same views of the 3D reconstruction results obtained using the optimized algorithm (e-h).

In Figures 5(e-h) different views of the reconstructed volume within the optimized FBA algorithm are presented. As one can see, the missing tooth is well resolved (see Figure 5(a)), and even the plane defects could be observed in the reconstruction (see Figure 5(j)). For better representation of the reconstruction results as well as to demonstrate the success of the reconstruction, slices of the model and the reconstruction are done in the xy-plane pathing through the defects and are presented in Figures 5(a, b), respectively.

Comparison of the model with the reconstruction demonstrates a good agreement of all defects with an acceptable resolution, which is confirmed by linear scans of the reconstruction and the model presented as insets in Figures 6(a, b). It is necessary to enhance ones again that the optical axis of the tomographic setup was shifted to the region of interest to implement the proposed scanning geometry. This condition is critical for the standard FBA approach, which requires the optical axis and the center of rotation to match. Therefore, the reconstruction results from the same scan with the standard algorithm completely fails in reconstruction presented for the comparison in Figure 6(c). However, the optimized version of the algorithm reconstructs the slice with a reasonable for the analysis quality (see Figure 6(b)).
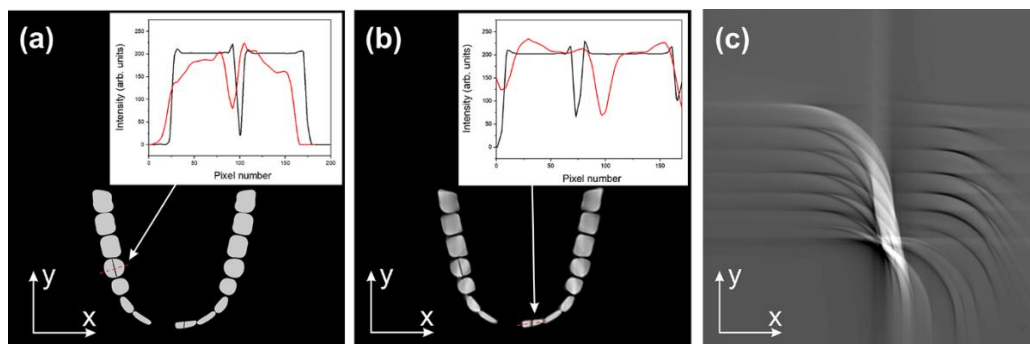


**Figure 6.** The 2D slice of the 3D teeth model in the xy-plane (a). The reconstruction results of this slice using the optimized reconstruction algorithm (b) and the standard FBA algorithm (c). The standard algorithm is not capable of reconstructing the sample. The efficiency of the optimized reconstruction is confirmed by linear scans of two defects of the reconstruction, and the model presented as insets in figures (a, b). Black lines correspond to the model and the red lines to the reconstruction.

We would like to underline ones again that some parts of the specimen in our study were unexposed. In the simulation, the skull and the teeth were assumed to be homogeneous with a mass attenuation coefficient of 0.4 cm$^2$/g adopted from the medical investigation of the bones at an energy of 50 keV [15, 16]. Further, we consider that the initial-amplitude level at the virtual detector represents the case when nothing stands on the X-ray beam path. Contrary, a pixel with zero value means full absorption of the X-ray beam and the maximum radiation dose absorbed. In the same way, any intensity level of the corresponding pixels can represent the dose obtained by the object with the specified maximum value depending on the chosen dynamical range of the image. Based on this assumption, we evaluated the decrease of the radiation dose for the 3D model of the skull with the teeth. The dose reduction reached a level of 64% in the case of the proposed scanning approach in comparison to the standard scan. It is possible to achieve such a decrease of the radiation dose by avoiding the illumination of the significant part of the scanning object. In our numerical experiment, the human head was simply unexposed by the X-rays.

The proposed modified scan could be realized by a combined optical and X-ray system with an optical camera positioned near the X-ray detector. The object under investigation should be first fixed and positioned approximately in the center of rotation of the detection system. Then, the optical camera should make several photos of the specimen at different angular positions e.g. 0 and 90 degrees. From the optical images, a ROI of the sample should be chosen manually by an operator or automatically by

a program. After the ROI position is defined, the center of rotation of the X-ray source and the detector should be shifted to its center, and the X-ray beam should be collimated to the ROI size. Further, the proposed above scan of the ROI could be performed.

## 4. Conclusion
Optimization of the standard tomographic CT scanning technique was proposed to decrease the radiation dose significantly by collimated X-ray beam illumination of only a region of interest of a specimen. Additionally, an optimization of the reconstruction algorithm was presented.

Applicability of the proposed scanning method was demonstrated on a simple 2D phantom and was further extended for a 3D model of a skull with teeth including different spatial defects. Numerical simulations demonstrated the success of the proposed method and allowed reconstruction of the models in 2D and 3D with an acceptable for medical application resolution, while the standard algorithm fails to demonstrate a reasonable reconstruction. We also estimated the dose reduction due to the modification of the scanning approach, which is a complicated function of the specimen and the region of interest, to be about 60%.

We hope that the results of our study, as well as the proposed approach, can contribute to the development of the next-generation medical X-ray tomographic setups with a significantly lower radiation dose.

## Acknowledgements

## References

[1]    Baruchel J, Buerre J Y and Maire E 2000 *X-ray tomography in material science* (Hermes science publications, France)
[2]    Russo P 2018 *Handbook of X-ray Imaging: Physics and Technology* (CRC Press)
[3]    H. E. M., C. M. L., D. J. S. and P. J. S. 2016 *X-ray Imaging: Fundamentals, Industrial Techniques and Applications* (CRC Press)
[4]    Hiller J, Maisl M and Reindl L M 2012 Measurement Science and Technology **23**
[5]    Hsieh J 2015 *Computed Tomography: Principles, Design, Artifacts, and Recent Advances, Third Edition* (SPIE Digital Library)
[6]    Kim D, Kim D, Yun J, Ha S, Kim S, Youn H and Kim H 2018 *IEEE Transactions on Nuclear Science* **65** 1180
[7]    S_lusarczyk Kacprzyk W, Skrzyn_ski W, Fabiszewska E and Bulski W 2011 *Radiation Protection Dosimetry* **147** 126
[8]    Matkevich E 2017 *PhD thesis*, Moscow State University of Medicine and Dentistry. A.I. Evdokimova
[9]    Herman G 2009 *Fundamentals of Computerized Tomography* (New York: Springer Publishing Company)
[10]   Kak A and Slaney M 2001 *Principles of Computerized Tomographic Imaging* (Philadelphia: SIAM)
[11]   Ozdiev A H, Afornu B K and Sednev D A 2018 *Research in Nondestructive Evaluation* **30(3)** 179-87
[12]   Gruzman I, Kirichuk V, Kosykh V, Peretyagin G I and Spektor A 2002 *Digital Processing of lmages in Information System* (Novosibirsk State Tech. Univ.)
[13]   Freud N, Duvauchelle P, L_etang J and Babot D 2006 *Nucl. Instr. Meth. Phys. Res.* **248** 175
[14]   Feldkamp L A, Davis L C and Kress J W 1984 *J. Opt. Soc. Am.* A **1** 612
[15]   White D R, Booz J, Gri_th R V, Spokas J J and Wilson I J 1989 *Journal of the International Commission on Radiation Units and Measurements* **os23**, NP
[16]   Estrela C, Bueno M R, Leles C R, Azevedo B and Azevedo J R 2008 *Journal of Endodontics* **34**